For reprint orders, please contact:
reprints@futuremedicine.com

CASE REPORT

New approach to radiation burn treatment by dosimetry-guided surgery combined with autologous mesenchymal stem cell therapy

JJ Lataillade[1†], C Doucet[1*], E Bey[2], H Carsin[2], C Huet[3], I Clairand[3], JF Bottollier-Depois[3], A Chapel[3], I Ernou[1], M Gourven[1], L Boutin[1], A Hayden[4], C Carcamo[4], E Buglova[5], M Joussemet[1], T de Revel[2] & P Gourmelon[3]*

[†]Author for correspondence
[1]Centre de Transfusion Sanguine des Armées, Jean Julliard, Unité de Thérapie Cellulaire, BP 410, 92141 Clamart Cedex, France
E-mail: jjlataillade@ctsa-armees.fr
Tel.: +33 141 467 260; Fax: +33 146 388 287
[2]Hôpital d'Instruction des Armées, Percy, BP 410, 92141 Clamart Cedex, France
[3]Institut de Radioprotection et de Sûreté Nucléaire (IRSN), BP 17, 92262 Fontenay aux Roses Cedex, France
[4]Hospital Mutual de Seguridad, Av. Lib. Bernardo O'Higgins 4848 Santiago, Chile
[5]International Atomic Energy Agency, Wagramer Strasse 5, P.O.Box 100, A-1400 Vienna, Austria

**These authors have equally contributed to this work*

The therapeutic management of severe radiation burns remains a challenging issue. Conventional surgical treatment (excision and skin autograft or rotation flap) often fails to prevent unpredictable and uncontrolled extension of the radiation necrotic process. We report here an innovative therapeutic strategy applied to the victim of a radiation accident (December 15, 2005) with an iridium gammagraphy radioactive source (^{192}Ir, 3.3 TBq). The approach combined numerical dosimetry-guided surgery with cellular therapy using mesenchymal stem cells. A very severe buttock radiation burn (2000 Gy at the center of the skin surface lesion) of a 27-year-old Chilean victim was widely excised (10 cm in diameter) using a physical and anatomical dose reconstruction in order to better define the limit of the surgical excision in apparently healthy tissues. A secondary extension of the radiation necrosis led to a new excision of fibronecrotic tissues associated with a local cellular therapy using autologous expanded mesenchymal stem cells as a source of trophic factors to promote tissue regeneration. Bone marrow-derived mesenchymal stem cells were expanded according to a clinical-grade technique using closed culture devices and serum-free medium enriched in human platelet lysate. The clinical evolution (radiation pain and healing progression) was favorable and no recurrence of radiation inflammatory waves was observed during the 11 month patient's follow-up. This novel multidisciplinary therapeutic approach combining physical techniques, surgical procedures and cellular therapy with adult stem cells may be of clinical relevance for improving the medical management of severe localized irradiations. It may open new prospects in the field of radiotherapy complications.

Keywords: accidental irradiation, mesenchymal stem cell, radiation burn, tissue regeneration

The medical management of severe radiation burns after accidental overexposure to ionizing radiation is still a major therapeutic challenge unresolved with the classical therapeutic approach derived from the management of thermal or electrical burns [1,2].

There are marked differences between radiation and thermal burns in terms of physio–pathological mechanisms, clinical aspects and evolution. The main feature of severe radiation burns is the occurrence of unpredictable successive inflammatory waves leading to the extension, in surface and in depth, of the necrotic process. After an initial period marked by a clinical picture limited to a rash and itching, subsequent ulceration and necrosis develop, which may extend to the deep dermal and underlying muscle structures [3]. Moreover, these inflammatory waves are associated with uncontrollable pain highly resistant to morphinics. The patho-physiological process, which implies a cascade of inflammatory mediators and a continuous activation of target cells (endothelial cells and fibroblasts) is not yet established. At very high radiation dose, this uncontrolled and extensive morbid process involves several target tissues including muscles, vessels and bones.

Presently, the classical treatment of radiation burns has remained conservative in the case of superficial lesions of distal extremities, with the use of necrectomy followed by rotation flaps and, in the case of profound and large necrosis, excision and coverage of the wound bed with a good quality, full-thickness skin graft. When new inflammatory waves impair this therapeutic approach, there has been no other approach than new extensive surgical excisions ending with successive amputations [4]. In all cases, the healing has been delayed, fragile and unpredictable [5,6]. As a result, severe radiation burns remain a highly puzzling and challenging therapeutic issue.

In the framework of a recent radiation accident concerning a 27-year-old Chilean man who had been overexposed to a gammagraphy radioactive source, we used an innovative therapeutic strategy combining both early dosimetry-guided lesion excision and cellular therapy with mesenchymal stem cells (MSCs). The aim of the early

10.2217/17460751.2.5.785 ISSN 1746-0751

dosimetry-guided surgery was to perform the most accurate and largest excision in order to prevent the vicious circle induced by the successive inflammatory waves reaching apparently healthy surrounding tissues. The aim of the MSC therapy was to deliver to the lesion site trophic factors able to favor the healing of the impaired tissue.

We report here on the favorable outcome of the radiation lesions following this therapeutic approach.

Case report & methods

Patient & irradiation accident

A 27-year-old Chilean man was overexposed, on 15 December 2005, to a gammagraphy radioactive source (^{192}Ir, 3.3 TBq). He picked up the source with his left hand and put it in the back left pocket of his trousers, where he kept it for approximately ten minutes before the alert was given. Following a multifocal localized irradiation, he rapidly exhibited severe radiation burns located to the hand and the buttock. The early occurrence of skin lesions (ringed permanent erythema with a central atonic area) at the buttock level within the first days after irradiation strongly suggested a very high-dose exposure. Following the request of the Chilean authorities through the International Atomic Energy Agency (IAEA) the patient was hospitalized at the Burn Treatment Centre (BTC) of Percy Military Hospital (Paris, France) on 29 December, 2005. The buttock skin lesion evolved into moist epidermitis (4–5 cm in diameter), then quickly worsened

Figure 1. Physical and anatomical dose reconstruction for surgical excision planning.

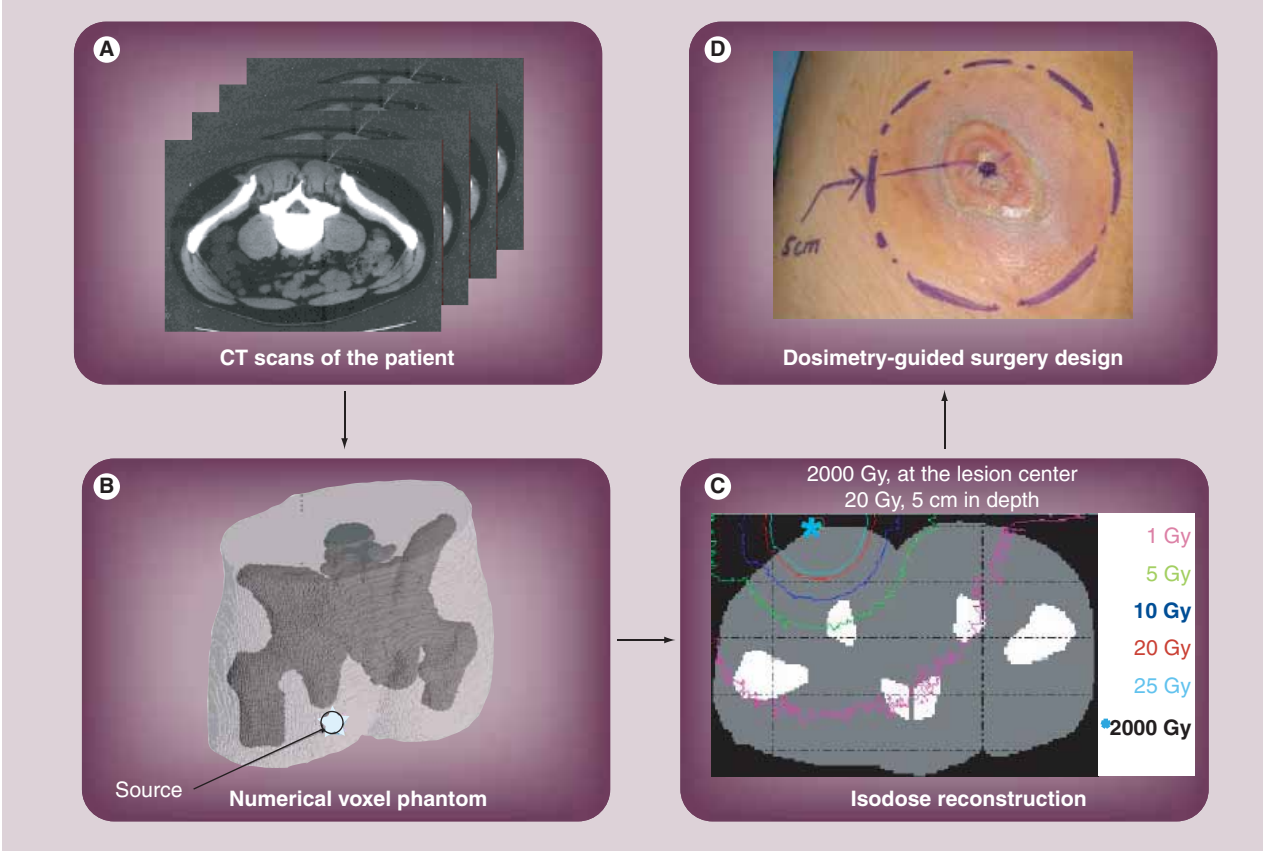

(A) CT scans of the patient: 163 slices from mid-abdomen to mid-thigh were used to generate a personalized numerical voxel phantom representative of the patient. **(B)** View of the voxel phantom of the victim with the source. Using SESAME software, a voxel phantom with external contours and bone structures was generated and the ^{192}Ir source was positioned at 2 mm from the center of the skin lesion surface on the left buttock. **(C)** Dose distribution pattern obtained at the same level as the source plane: a map of the dose distribution on the skin surface and underlying tissues of the buttock was obtained with numerical simulations associating a Monte Carlo code and the personalized voxel phantom. The dose absorbed at the skin surface is very high (almost 2000 Gy). The gradient of the dose was very sharp: the 20 Gy and 5 Gy isodoses were respectively situated at 5 cm and 10 cm from the centre of the lesion. **(D)** Dosimetry-guided surgery: based on this mapping, a surgical excision measuring 10 cm diameter in surface and 5 cm in depth was performed on the left buttock. CT: Computed tomography.

and progressed to ulceration. In the weeks following exposure, the left hand exhibited erythematous lesions with swollen fingers. These radiation skin lesions were accompanied by classical intense pain, which was only partially alleviated by morphine. The early development of the buttock lesion without any latency phase, its fast evolution toward ulceration and the uncontrolled pain were characteristic of a very severe radiation burn with poor prognosis.

Physical dosimetric reconstruction

The strategy adopted to reconstruct the accidental dose distribution delivered to the patient was based on numerical simulations. A numerical dosimetric reconstruction of a radiation accident needs to simulate the source, its environment and the patient body using a numerical anthropomorphic phantom. The doses absorbed by the tissues are then calculated using a computer code. Such numerical methodology was recently applied to other severe radiation accidents [7,8]

In this accident a voxel anthropomorphic phantom was used and generated with the SESAME software [9] from 163 computed tomography slices (mid-abdomen to mid-thigh) (Figure 1A & 1B). The simulations were carried out assuming an exposure time of 10 min and an activity of ^{192}Ir of 3.3 TBq. Calculations were performed to generate a map of the dose distribution on the skin surface and underlying tissues of the buttock using the MCNPX version 2.4.0 Monte Carlo code [10]. This code is widely used in dosimetry assessment to model the transport and interaction of charged or neutral particles in matter.

Autologous mesenchymal stem cells production

The patient gave written consent for a new therapeutic strategy combining a surgical approach and MSC local therapy. Ethical and technical approvals were obtained from the French health authority (AFSSaPS). Autologous bone marrow total cells (BMCs) were obtained from unexposed iliac crest aspirations. A novel clinical-grade MSC production process using closed culture devices (Cellstack®, Corning, Macopharma, Tourcoing, France) was used. Cells were expanded in a clinical grade medium containing α-MEM (Macopharma), 10 µg/ml ciprofloxacin (Ciflox® 400 mg/200 ml, Bayer Pharma, Puteaux, France) and 8% human platelet lysate (PL) as a source of growth factors [11,12]. PL were obtained from platelet apheresis products that were biologically qualified according to French legislation. The platelet number of each product was automatically measured (ADVIA 120, Bayer) and only samples containing approximately 1.10^9 platelets/ml were selected and frozen at -80°C to obtain a PL containing platelet-released growth factors. PL products were then thawed and harvested to be used in culture as fetal calf serum (FCS) substitutes. 254.5×10^6 BMCs were plated at a density of 200×10^3 cells/cm^2 on day 75 postirradiation (PI) in 1272 cm^2 Cellstack® devices containing PL medium and cultured at 37°C in 95% air and 5% CO_2. After 3–4 days, the nonadherent cells were removed and the cultures were re-fed with fresh medium. On day 14 after the start of the culture, cells reached confluence. One part of MSCs was harvested after a 1× trypsin-ethylenediamine tetraacetic acid (EDTA) (both from Sigma) application for 5 min at 37°C, conditioned in human albumin and freshly administered. 10×10^6 of remaining MSCs were reseeded at a density of 8×10^3 cells/cm^2 in two 1272 cm^2 Cellstack® and 7 days later, P2 MSCs were harvested for the second local administration.

Quality controls were achieved on each cell product:

- MSC phenotype characterization (CD45$^-$/CD105$^+$/CD73$^+$/CD90$^+$) as previously described [11].
- Colony-forming unit-fibroblast (CFU-F) frequency numeration: briefly, 0.33×10^6 BMCs were cultured in 25 cm^2 flasks with PL medium. The medium was replaced every 3 days and cultures were stopped on day 10. Next, the cell layer was fixed and stained with a Giemsa solution at pH 7 (Biolyon, Dardilly, France). Clonogenic efficiency was calculated as number of colonies per 10^6 cells seeded.
- MSC telomerase activity was performed using a modified telomeric repeat amplification method (TRAP assay) described by Kim NW *et al.* [13]. A TeloTAGGG Telomerase PCR ELISAPLUS detection kit (Roche Applied Science) was used to quantify telomerase activity according the manufacturer recommendations.
- Before administration contamination control for bacteria, fungi and mycoplasma.

Histological analysis

Histological examination of 5 µm tissue section of skin and muscle excisions was performed after fixation in 5% formaldehyde and staining with hematoxylin-eosin.

Figure 2. Surgical therapy.

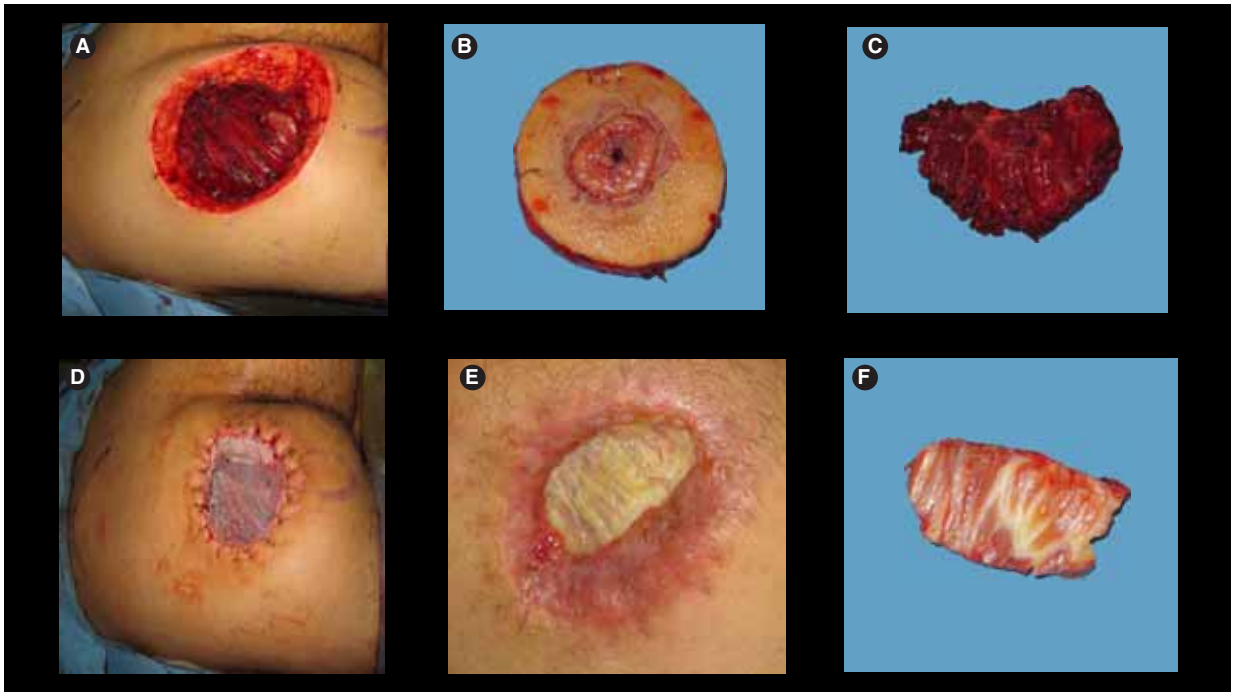

The wide surgical excision of the buttock radiation burn was performed on day 21 PI according to the anatomical and physical dose reconstruction. **(A)** View of the excision (10 cm diameter). **(B)** Excised cutaneous and subcutaneous tissues including the central radiation burn. **(C)** Excised gluteal muscle in apparent healthy status. The excision was followed by a temporary wound closure with a cryopreserved skin allograft **(D)** and in a second step, by a skin autograft (day 49 PI). The clinical evolution was marked by a lysis of the skin graft and a recurrence of a fibro-necrotic process in the bottom of the wound – day 90 PI **(E)**. An additional surgical excision of the muscular fibrotic tissue was applied **(F)** and followed by a second skin autograft at day 90 PI.
PI: Postirradiation.

Results

Dose reconstruction of the buttock lesion

A dose reconstruction of the radiation lesion using numerical method and taking into account the anatomical characteristics of the patient was performed in order to improve the accuracy of the surgical excision. The dose distribution obtained with numerical simulations associating a Monte Carlo code and a Voxel phantom representative of the patient anatomy is illustrated in Figure 1C. The dose absorbed at the skin lesion center was very high (almost 2000 Gy), but dropped rapidly due to the combined effect of distance and tissue attenuation. Thus, the 20 Gy and 5 Gy isodoses were respectively situated at 5 cm and 10 cm from the center of the lesion.

Dosimetry-guided surgery

Based on the dose reconstruction mapping, a wide resection in apparently healthy tissues was performed on day 21 PI (Figures 1D & 2A, B, C). All tissues exposed to a dose over 20 Gy that were situated between the center of the lesion and the 20 Gy isodose were excised according to hemisphere of 10 cm in diameter and then covered with a cryopreserved allograft (Figure 2D). Histological examination of excised cutaneous tissues revealed characteristic histological features of skin burns (Figures 3B, C & D). The center of the lesion was characterized by both dermal ulceration and marked epidermolysis (Figure 3D). Complete disjunction of the epidermis with germinal and keratinocyte interphase cell death associated with a loss of epidermis adhesiveness to the basal layer were observed (Figure 3C). Concerning the underlying muscular structure, morphology of the striated muscle was quite normal without any sign of rhabdomyolysis, with discrete fibroadipocytic intensification punctuated with small vessels and normal morphological nervous structure.

Following surgery, no infection or subsequent radiation inflammatory wave was observed for 1 month. Due to this apparent normal evolution, a skin autograft was performed on day 49 PI. Rapid lysis of the skin graft occurred with the development of a painful infected radiation ulceration (Figure 2E).

Figure 3. Histological characteristics of radio-induced tissue damages.

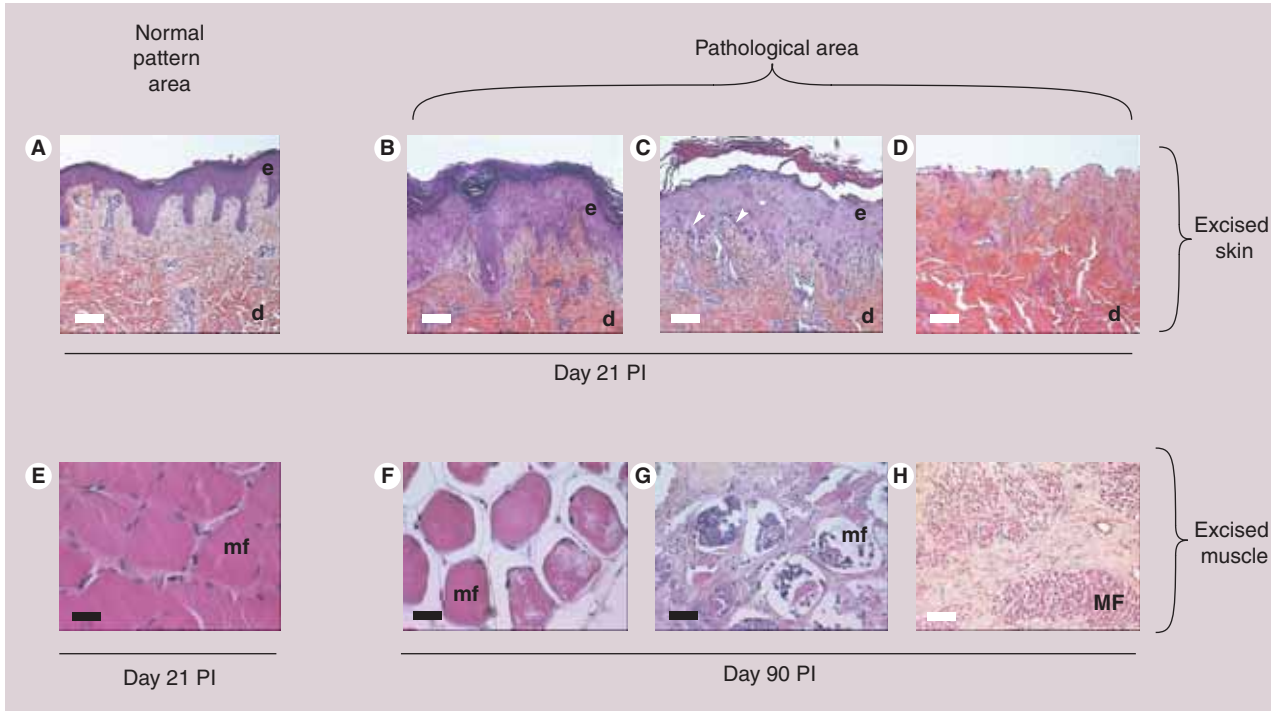

Transverse sections of skin **(A–D)** and muscle **(E–H),** 21 days **(A–E)** or 90 d **(F–H)** postirradiation in normal **(A,E)** or pathological **(B–D; F–H)** areas.
Scale bars: 100 μm for A–D and H pictures (white bar) and 25 μm for E–G pictures (black bar).
White arrow heads (panel C): basal layer disjunction.
d: Dermis, e: Epidermis, mf: Muscular fiber, MF: Muscular fasciculus; PI: Postirradiation.

New therapeutic approach with cell therapy

A new therapeutic strategy combining a classical surgical therapy (excision plus skin autograft) and a local MSC therapy was designed (Figure 4). For MSC production, an autologous bone marrow collection was performed, allowing a two-step MSC expansion producing 182×10^6 cells at the first passage (P1) and 227×10^6 cells at the second passage (P2). Results of cell production are summarized in Table 1. Expanded cells exhibited antigenic characteristics of MSCs: they did not express CD45, but expressed CD90, CD105 and CD73 antigens (Figure 5). MSC purity was up to 97% and their clonogenic efficiency obtained at P1 was 225. No telomerase activity was found in the expanded MSCs (Table 1). The pluripotentiality of expanded MSC was controlled by *in vitro* osteogenic, adipogenic and chondrogenic assays performed on five preclinical culture runs (data not shown).

The first step of this therapeutic approach was the surgical excision of the muscular fibrotic tissue, followed by a second skin autograft (Figure 2F). Histological examination of muscle resection revealed characteristic features of radiation burn recurrence (Figures 3F, G & H). Muscular injury was very heterogeneous and started with degeneration and retraction of muscular fibers (Figure 3F). Some areas were characterized by fibro-atrophic lesions with compression of number of muscular fasciculus (Figure 3H) evolving sometime into rhabdomyolysis with numerous plurinucleated cells (Figure 3G). Fibrosis is punctuated by some inflammatory mononucleated cells. Vascular damages were remarkable by their polymorphism, their focal characteristic and the absence of systematization. Fibrinoid necrosis of the vascular wall was associated with perivascular inflammatory cell infiltration. Swollen endothelial cells were associated with polynuclear wall infiltration, and fibrinous thrombi obstructing the vessel lumen were observed.

The second therapeutic step was the local administrations of 168×10^6 MSC on day 90 PI (Figure 4A) and 226×10^6 on day 99 PI (Figure 4D), which were injected in circle around the lesion at the cutaneous and muscular levels, and in the wound bed of the lesion under the skin graft. The lesion was further dressed with an artificial

Figure 4. Mesenchymal stem cell therapy.

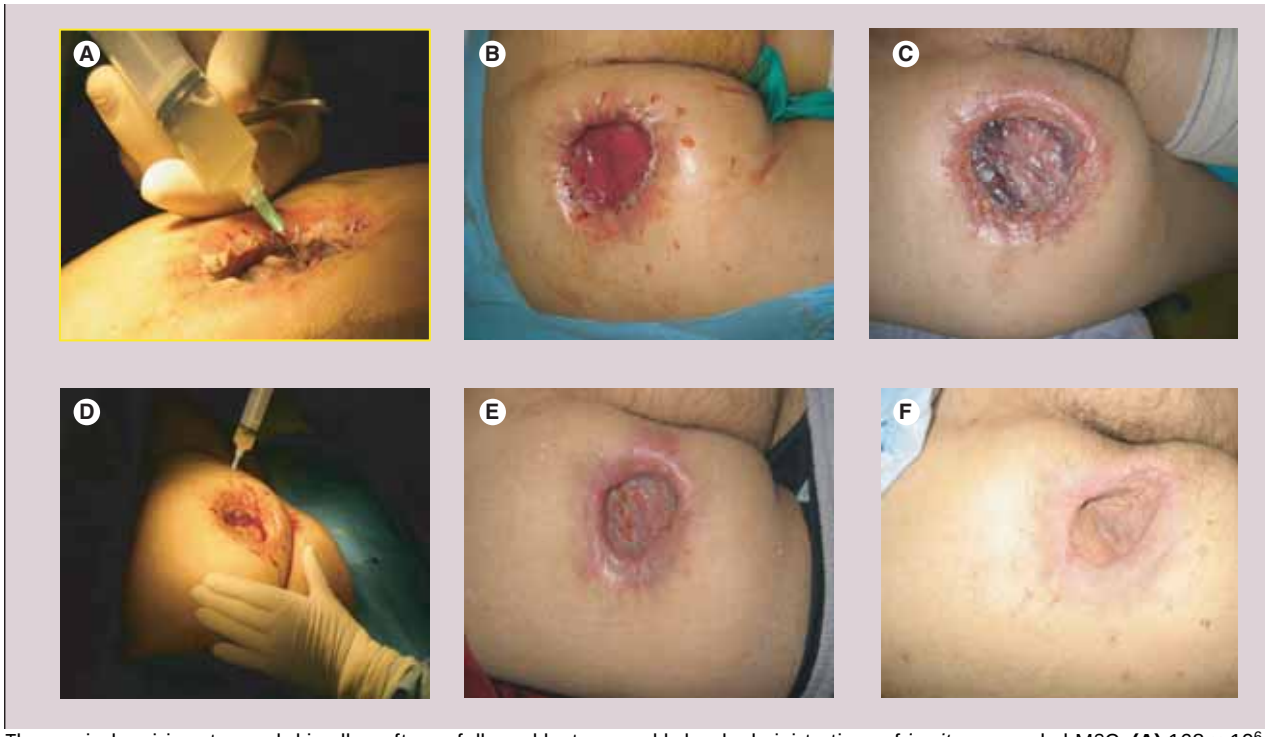

The surgical excision step and skin allograft was followed by two weekly local administrations of *in vitro* expanded MSC. **(A)** 168 × 10^6 MSC were injected on day 90 PI in a circle around the lesion and into the wound bed. **(B)** The lesion was further dressed with an artificial derma (Integra®). **(C)** View of the lesion 9 days after the first MSC administration. **(D)** 226 × 10^6 MSC were injected on day 99 PI in a circle around the lesion at the cutaneous and muscular levels. **(E)** Healing evolution on day 109 PI. **(F)** Final aspect of the lesion (5.5 months PI)
MSC: Mesenchymal stem cells; PI: Postirradiation.

derma (Integra®) (Figure 4B). Figure 6 shows a schematic temporal pattern of successive surgical and cellular therapies.

Evolution

Following this therapy combining surgical excision and cell administration, no adverse reaction to the autologous MSC administration was observed. The day following the MSC injections, pain disappeared and the active clinical evolution of the radiation burn was stopped. The healing of the lesion was ascertained by the quality of the engraftment. Unlike the classical evolution of a very severe radiation skin lesion, the size of the wound progressively decreased following a centripetal process (Figures 4E & F). Almost complete healing was achieved by 1 month post-treatment.

No recurrence of radiation burn was observed during the follow-up of the patient. The healing was complete without any functional impairment at 5.5 months post irradiation (day 75 post-cell therapy). The only persistent sequelae were aesthetic (Figure 4F).

Discussion

In contrast to thermal burns, radiation burns exhibit several clinical patterns including dry desquamation, moist desquamation and necrosis according to the radiation dose level [3,4].

Dry and moist desquamations are skin clinical manifestations of the keratinocyte mitotic death and necrosis is the consequence of the tissue radiation injuries that have reached not only the skin, but also the deep subcutaneous structures such as muscles, vessels and sometimes even bone [5].

The surgical management of severe necrotic radiation burns is theoretically easy to perform. The conventional main strategy is the excision of the necrotic tissues followed by a rotation flap or a good quality skin autograft. In practice, the planning of such a surgical approach often encounters insurmountable technical difficulties due to the occurrence of successive and unpredictable inflammatory waves associated with a progressive extension of the necrotic process [6]. Then, the evolution of the radiation lesion often becomes uncontrolled and the final option is a last surgical act leading to a

Figure 5. Mesenchymal stem cell phenotype characterization.

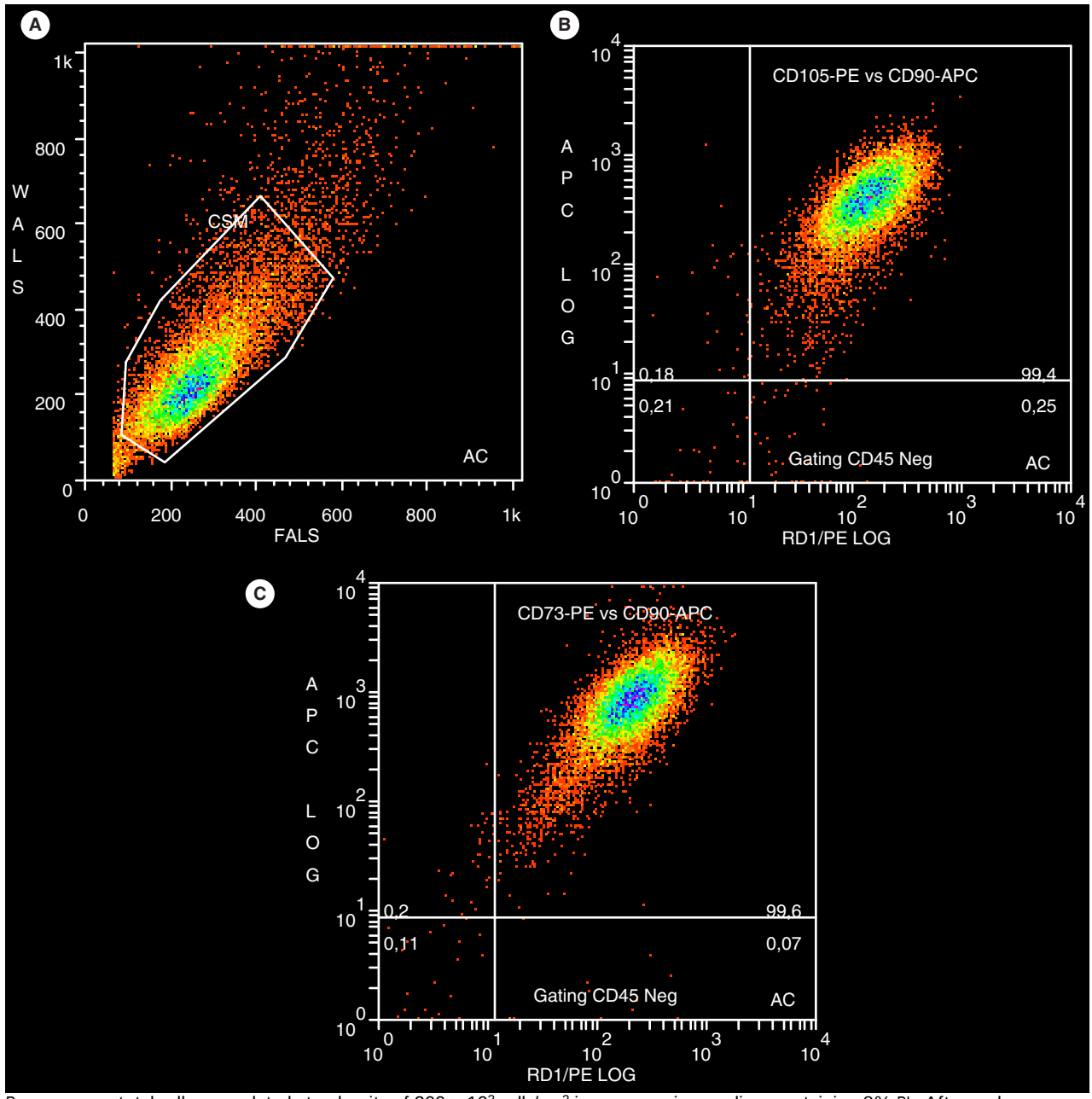

Bone marrow total cells were plated at a density of 200 × 10^3 cells/cm^2 in an expansion medium containing 8% PL. After each passage, the cells were assessed for antigenic expression by flow cytometry. Cells were labeled with antibodies against CD45, CD90, CD105, and CD73 or control IgGs, and analyzed by flow cytometry. Plots show specific antibody staining profiles for cells cultured in PL at passage 2 **(B & C)** CD45 negative cells were analyzed for CD90, CD73 and CD105 expression by three-color flow cytometry.
PL: Platelet lysate

very high morbidity and disability [6]. Thus, in two highly irradiated Peruvian and Georgian victims that we previously treated in 1999 and 2002 with the classical surgical approach combining excision and skin graft, we were unable to control, in the Peruvian case, even after amputation of the irradiated leg, the huge extension, at the perineal level, of the radionecrotic process. Concerning the Georgian case, the conventional treatment was a failure since four successive excisions followed by skin autografts were always inefficient 440 days post-exposure and only an autonomous, vascularized tissue (omentum flap) covered by skin allograft allowed healing at 500 days PI (Table 2).

Table 1. MSC production rates and quality controls.

	Passages	
	P1	***P2***
Bone marrow aspiration (ml)	25	-
Input of BMMNCs and MSCs*	254.5×10^6	10×10^6*
Total MSC production	182×10^6	227×10^6
Culture duration (days)	14	7
MSC purity (%)	97	100
CFU-F efficiency (per 10^6 cells seeded)	225	-
Telomerase activity	None	None
Micro-organism contamination	Negative	Negative
Number of MSCs injected (day PI)	168×10^6 (90)	226×10^6 (99)

BMMNC: Bone marrow mononuclear cells; CFU-F: Colony-forming unit-fibroblast; MSC: Mesenchymal stem cells.

Thus, to date, the best therapeutic approach for severe radiation burns remains unknown.

One of the unsolved issues is the size of the excision surgery. Indeed, in a classical surgical approach, the limits of any lesion to be removed are well defined. By contrast, regarding radiation burns, the actual limits of the lesion are unknown and a tissue that may appear at first healthy may in fact necrose more or less rapidly. The first challenge for the surgeon is to appreciate the boundaries between healthy and injured tissues. The unique way to get reliable information concerning this invisible limit is to know the gradient of dose delivered to the tissues. The necrotic process is known to occur in tissues that received a dose greater than 25 Gy.

We took advantage in this accident of the early recognition of the event with a clear description of the circumstances, so that we were able, for the first time in a radiation burn victim, to do a physical dosimetric reconstruction to guide the surgical excision.

In practice, physical dose reconstruction with numerical methods requires a perfect knowledge of key parameters such as the activity of the source, the position of the source, the distance between the source and the lesion, and the duration of the exposure.

In the present case, several parameters were crucial for assessing an accurate dose reconstruction. Indeed, the accidental scenario was very precise, the activity of the source was well known, the source was wedged in a rear pocket trouser and was not moved during the exposure, constantly almost in direct contact with the skin. Moreover, the most subjective parameter of a dose reconstruction, which is the time of exposure, was pretty well quantified by the victim himself (10 min by watch checking) in this case. In addition, the physical dose reconstruction was carried out from a personalized voxelized phantom generated from the tomodensitometric images of the victim. The dose reconstruction mapping confirmed the very high severity of the local irradiation since 2000 Gy was delivered to the center of the lesion. The main characteristic of a ^{192}Ir source irradiation is the very sharp gradient of dose delivered inside the target tissue. The 25 Gy necrotic boundary isodose was situated at 4.5 cm in depth from the center of the skin surface lesion. The key issue of an accidental dose reconstruction is the assessment of uncertainties that are in practice very difficult to quantify. Consequently, a safety factor of 20% was applied for the dosimetry-guided surgery and the 20 Gy isodose was defined as the limit of the excision in surface (10 cm in diameter) and in depth (5 cm). Postsurgical follow-up demonstrated that this anatomical dose assessment was effective in surface, but could have been underestimated in depth as suggested by the recurrence of the radiation muscular lesion focalized in the wound bed. Another hypothesis could be the technical difficulty in controlling accurately the depth of the surgical excision. Last, a high radiosensitivity of the patient could also be suspected in view of the occurrence of the muscular fibrotic process and the lysis of the autograft.

The present accident demonstrates one more time that in case of a very severe radiation burn, the classical therapeutic strategy (serial excisions followed by skin autografts) is inappropriate. Therefore, following this primary failure, we decided to design an innovative therapeutic approach with cellular therapy.

Figure 6. Schedule of dose assessment, surgical and cellular therapeutical approaches.

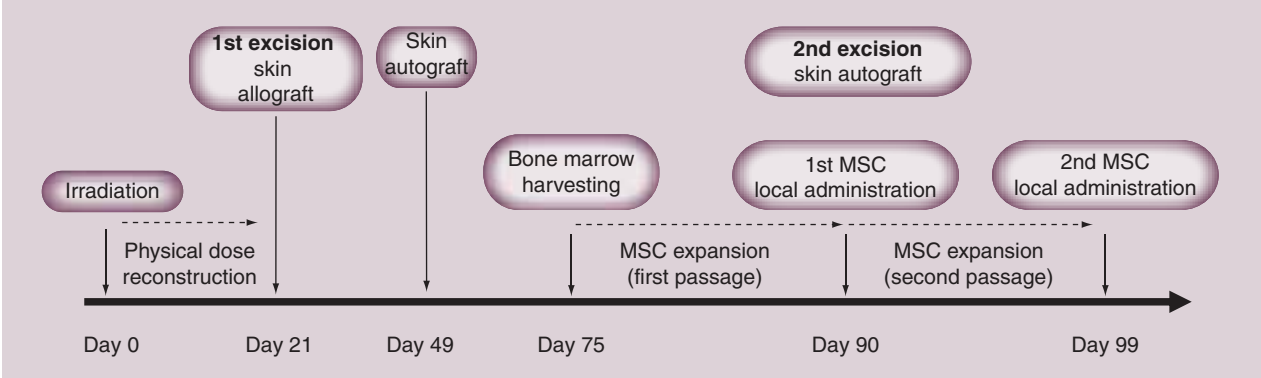

MSC: Mesenchymal stem cells.

MSCs are defined as pluripotent cells capable of proliferating extensively and able to give rise to skeletal tissues: bone, cartilage, tendon and marrow stroma [14–16]. Moreover, MSCs are able to migrate towards injured tissular lesions where they deliver a high number of growth factors that are required for immunoregulation and repair processes [17–19]. It has been demonstrated that MSCs can be easily recovered from bone marrow and enriched through their property of adhering to tissue culture surfaces [20]. Several teams have recently expanded MSCs up to a millionfold *in vitro* for hematologically and orthopedically relevant applications [21–24]. We have previously shown their positive effect in promoting the healing of radiation burn lesions in a preclinical immunodeficient nonobese diabetic/severe combined immunodeficient (NOD/SCID) mouse model: in this model, the intravenous administration of human MSCs strongly improved the healing of burn lesions of the leg induced by a 30 Gy irradiation [25]. In this context we proposed to the patient a new therapeutic approach where the second surgical excision and skin graft was locally combined with the use of MSC therapy.

Muscular fibrotic tissues were again excised, and a new skin autograft performed. Expanded bone marrow-derived MSC were locally injected around and in the lesion and this was repeated a week later. Following this combined therapy, the healing of the lesion proceeded smoothly. There was no side effect. Perfect healing persists 1 year after the procedure.

We postulate that MSC favored the radiation burn healing process through the secretion of soluble mediators (cytokines) and trophic factors that may have counteracted the local inflammatory wave processes [25,26]. However, we had no way to study the fate of the infused MSCs because of their autologous nature and the lack of specific markers. It has been shown recently in several studies with MSCs that when their presence can be detected at some tissue sites, this usually does not last over 6–9 months [23].

Table 2. Comparative therapeutic strategies of very severe radiation burns in three historical cases.

	Radiation burn localization (size)	Surgical treatment strategy: excision, artificial skin graft, skin autograft, omentum flap			Mesenchymal stem cell therapy	Final outcome
Peruvian case (1999)	Right thigh (30 × 13 cm)	2 excisions	Excision + sciatic nerve cutting	Lower limb amputation	No	No healing (extension to perineum area)
Georgian case (2002)	Back (26 × 19 cm)	Excision + artificial skin graft	4 excisions + 4 skin autografts	Excision + omentum flap + skin autograft	No	Healing (16.5 months post-treatment)
Chilean case (2005)	Left buttock (5cm in diameter)	2 excisions + 2 skin autografts	2 excisions + 2 skin autografts	2 excisions + 2 skin autografts	2 MSC local administrations	Healing (5.5 months post-treatment)

In conclusion, we present this report as possibly indicating the efficacy of human MSC therapy in the management of very severe radiation burns involving cutaneous and subcutaneous structures. If confirmed in further radiation accidents, which fortunately by nature are rare although dramatic events, it would bring a major therapeutic improvement. Furthermore, this novel multidisciplinary therapeutic approach using physical techniques, surgical procedures and cellular therapy with adult stem cells may open new prospects in the field of radiotherapy complications.

Financial disclosure

The authors have no relevant financial interests, including employment, consultancies, honoraria, stock ownership or options, expert testimony, grants or patents received or pending, or royalties related to this manuscript.

Acknowledgements

The authors thank Valerie Buard and Valerie Holler for their histological technical assistance.

Bibliography

1. Gottlöber P, Bezold G, Weber L *et al.*: The radiation accident in Georgia: Clinical appearance and diagnosis of cutaneous radiation syndrome. *J. Am. Acad. Dermatol.* 42, 453–458 (2000).
2. Peter RU, Gottlöber P: Management of cutaneous radiation injuries: diagnostic and therapeutic principles of the cutaneous radiation syndrome. *Mil. Med.* 167, 110–112 (2002).
3. Peter RU: Cutaneous radiation syndrome in multiorgan failure. *Br. J. Radiol.* 27(Suppl.), 180–184 (2005).
4. Zaharia M, Goans RE, Berger ME *et al.*: Industrial radiography accident at the Yanango hydroelectric power plant. In: *The Medical Basis for Radiation-Accident Preparedness.* The Parthenon Publishing Group, London, UK, 267–281 (2001).
5. Lefaix JL, Delanian S: Le syndrome cutané radio-induit. In: *The terrorist threat NUCLEAR, RADIOLOGICAL, BIOLOGICAL, CHEMICAL – A medical approach.* De Revel T, Gourmelon P (Eds), John Libbey Eurotext, Montrouge, France, 87–95 (2005).
6. Stephanazzi J, Bargues L, Curet PM, Lebevert H, Carsin H: Le traitement du syndrome cutané radiologique. In *John Libbey Eurotext. The terrorist threat Nuclear, Radiological, Biological, Chemical–A medical approach.* De Revel T, Gourmelon P (Eds). 112–122 (2005).
7. Clairand I, Trompier F, Bottollier-Depois JF, Gourmelon P: *Ex vivo* ESR measurements associated with Monte Carlo calculations for accident dosimetry: application to the 2001 Georgian accident. *Radiat. Prot. Dosimetry* 119, 500–505 (2006).
8. Bottollier-Depois JF, Gaillard-Lecanu E, Roux A, *et al.*: New approach for dose reconstruction: application to one case of localized irradiation with radiological burns. *Health Phys.* 79(3), 251–256 (2000).
9. Lemosquet A, Clairand I, de Carlan L, Franck D, Aubineau-Lanièce I, Bottollier-Depois JF: A computational tool based on voxel geometry for dose reconstruction of a radiological accident due to external exposure. *Radiat. Prot. Dosimetry* 110, 449–454 (2004).
10. Walters LS: MCNPX User's Manual, Version 2.4.0, LA-CP-02–408, Los Alamos National Laboratory, NM, USA (2002).
11. Doucet C, Ernou I, Zhang Y *et al.*: Platelet lysates promote mesenchymal stem cell expansion: a safety substitute for animal serum in cell-based therapy applications. *J. Cell. Physiol.* 205(2), 228–236 (2005).
12. Lange C, Cakiroglu F, Spiess AN, Cappallo-Obermann H, Dierlamm J, Zander A: Accelerated and safe expansion of human mesenchymal stromal cells in animal serum-free medium for transplantation and regenerative medicine. *J. Cell. Physiol.* 213(1), 18–26 (2007).
13. Kim NW, Piatyszek MA, Prowse KR *et al.*: Specific association of human telomerase activity with immortal cells and cancer. *Science* 266, 2011–2015 (1994).
14. Bentley SA: Bone marrow connective tissue and the haemopoietic microenvironment. *Br. J. Haematol.* 50(1), 1–6 (1982).
15. Caplan AI: Mesenchymal stem cells. *J. Orthop. Res.* 9(5), 641–650 (1991).
16. Ringden O, Uzunel M, Rasmusson I *et al.*: Mesenchymal stem cells for treatment of therapy-resistant graft-versus-host disease. *Transplantation* 81(10), 1390–1397 (2006).
17. Chapel A, Bertho JM, Bensidhoum M *et al.*: Mesenchymal stem cells home to injured tissues when co-infused with hematopoietic cells to treat a radiation-induced multiorgan failure syndrome. *J. Gene Med.* 5, 1028–1038 (2003).
18. François S, Bensidhoum M, Mouiseddine M *et al.*: Local irradiation not only induces homing of human mesenchymal stem cells at exposed sites but promotes their widespread engraftment to multiple organs: A study of their quantitative distribution after irradiation damages. *Stem Cells* 24, 1020–1029 (2006).
19. Le Blanc K, Ringden O: Mesenchymal stem cells: properties and role in clinical bone marrow transplantation. *Curr. Opin. Immunol.* 18(5), 586–591 (2006).
20. Friedenstein AJ, Gorskaja JF, Kulagina NN: Fibroblast precursors in normal and irradiated mouse hematopoietic organs. *Exp. Hematol.* 4(5), 267–574 (1976).
21. Koc ON, Gerson SL, Cooper BW *et al.*: Rapid hematopoietic recovery after coinfusion of autologous-blood stem cells and culture-expanded marrow mesenchymal stem cells in advanced breast cancer patients receiving high-dose chemotherapy. *J. Clin. Oncol.* 18(2), 307–316 (2000).
22. Horwitz EM, Prockop DJ, Fitzpatrick LA, *et al.*: Transplantability and therapeutic effects of bone marrow-derived mesenchymal cells in children with osteogenesis imperfecta. *Nat. Med.* 5(3), 309–313 (1999).
23. Le Blanc K, Rasmusson I, Sundberg B *et al.*: Treatment of severe acute graft-versus-host disease with third party haploidentical mesenchymal stem cells. *Lancet* 363(9419), 1439–1441 (2004).
24. Fouillard L, Bensidhoum M, Bories D *et al.*: Engraftment of allogeneic mesenchymal stem cells in the bone marrow of a patient with severe idiopathic aplastic anemia improves stroma. *Leukemia* 17(2), 474–476 (2003).
25. François S, Mouiseddine M, Mathieu N *et al.*: Human mesenchymal stem cells favour healing of the cutaneous radiation syndrome in a xenogenic transplant model. *Ann. Hematol.* 86, 1–8 (2007).
26. Thierry D, Bertho JM, Chapel A, Gourmelon P: Cell therapy for the treatment of accidental radiation overexposure. *Br. J. Radiol.* 27(Suppl.), 175–179 (2005).